Homologous Ladder Cyclohexasilanes

Fan Fang,[a] Andrew Molino,[b] Kelsie E. Wentz,[a] Carlton P. Folster,[a]† Jessica L. Williams,[a] Maxime A. Siegler,[a] Rebekka S. Klausen*[a]

[a] Mr. Fan Fang, Dr. Kelsie E. Wentz, Dr. Carlton P. Folster, Ms. Jessica L. Williams, Dr. Maxime A. Siegler, Prof. Rebekka S. Klausen
Department of Chemistry
Johns Hopkins University
3400 N. Charles St, Baltimore, MD, 21218, USA
E-mail: klausen@jhu.edu

[b] Dr. Andrew Molino
Department of Chemistry
Massachusetts Institute of Technology
77 Massachusetts Avenue, Cambridge, MA, 02139, USA

Supporting information for this article is given via a link at the end of the document.

Abstract: We report the synthesis of five new examples of ladder cyclohexasilanes, possessing up to three consecutive fused rings and differing in relative ring fusion configuration and side chain structure. By coupling a 1,4-dipotassiooligosilyl dianion to a cyclohexasilane, we obtained bi- and tricyclic ladder cyclohexasilanes. Combined experimental and theoretical studies suggested that annulation could favor the *cis* configuration under kinetic control, while the *trans* configuration predominates under thermodynamic control. Computational studies show that with each additional ring in the *trans*-diastereomeric series, the predicted onset of light absorption shifts to longer wavelengths.

Introduction

Ladder molecules and macromolecules feature two parallel chains of atoms formed by the consecutive fusion of two or more rings. This class of polycyclic compounds has long posed a significant synthetic challenge due to their architectural complexity and attracted interest for the unusual properties arising from their constrained conformations and restricted degrees of freedom.[1] Examples of carbocyclic ladder compounds include ladderanes, which possess both biological significance[2,3] and rich mechanochemically coupled cycloreversion chemistry,[4,5] fused cyclohexanes arising from Diels–Alder cycloadditions,[6,7] and conjugated acenes and heteroacenes.[8–10] Beyond carbon, inorganic examples of ladder covalent compounds are rare, while ladder-like coordination polymers,[11] polysiloxanes,[12] and minerals are better represented.[13] Matsumoto synthesized the smallest example of a ladder cyclosilane, the bicyclo[2.2.0]hexasilane, in 1987.[14] Speaking to the considerable challenge posed by these compounds, 20 years later Matsumoto reported that reductive coupling of linear dichlorosilanes affords complex mixtures of ladder polysilanes with between four to eight consecutive fused cyclotetrasilanes, from which individual examples could be isolated by recycling high-performance liquid chromatography.[15,16]

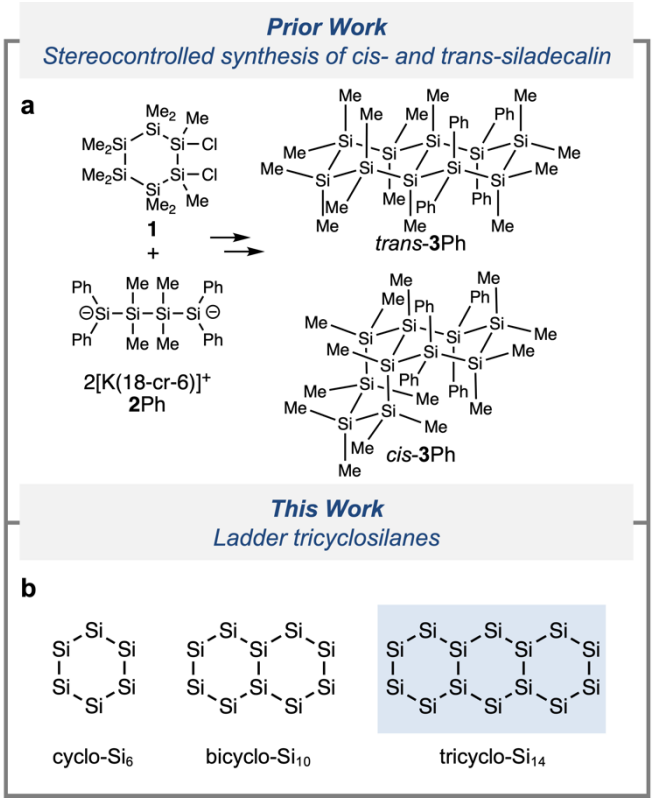

Scheme 1. A) Prior work: Synthetic access to diastereomeric siladecalins, the simplest ladder polymer of cyclohexasilane. B) This work: synthesis of a ladder tricyclosilane.

In 2019, we reported the stereocontrolled synthesis of both diastereomers of siladecalin **3**Ph (Scheme 1a), the smallest example of a ladder polysilane consisting of fused 6-membered rings.[17] The tetraphenyl siladecalins **3**Ph could be converted to the hydrido-functionalized siladecalins **3**H by protonolysis and reduction without erosion in relative configuration. We found that relative configuration influenced conformation-dependent absorbance spectra;[18] the rigid *trans*-siladecalin **3**H strongly absorbed UV light (λ ~ 270 nm), while the conformationally dynamic *cis* isomer did not. These insights sparked our interest in the next highest congener, a tricyclo-Si_{14} scaffold consisting of three fused cyclohexasilanes (Scheme 1b). At the same time, we appreciated that the extension of the ladder polysilane by just one additional ring would result in considerable additional complexity. While the siladecalin, or bicyclo-Si_{10}, exists in two diastereomeric forms, the tricyclo-Si_{14} has five possible diastereomers differing in the relative configurations at the ring fusions (Figure S1). The tricyclo-Si_{14} diastereomers are named following the convention developed for the carbocycle perhydroanthracene: *trans,syn,trans* (tst), *cis,trans* (ct), *trans,anti,trans* (tat), *cis,anti,cis* (cac), and *cis,syn,cis* (csc).[19,20]

Herein, we report the synthesis and isolation of four examples of ladder tricylohexasilanes possessing a core of 14 silicon atoms arranged in three consecutive fused rings while differing in the exocyclic substituents and relative configuration at the ring fusion. These ladder tricyclosilanes rank among the most complex oligosilanes yet synthesized,[21,22] based on size, multiple rings, and multiple stereogenic-at-silicon centers. We also report the stereoselective synthesis of an additional example of a siladecalin (bicyclo-Si_{10} compound, **3**TMS). Our results show that *cis* diastereoselectivity is enhanced under kinetic control, while thermodynamic control increases the yield of *trans* configurations. We expect these results to inform the emerging area of stereoselective synthesis at silicon and other main group centers[23–29] by providing examples of configuration-dependent properties that could inform target and substrate design, as well as insight into reaction conditions that could result in unexpected racemization. We also find computationally that as the number of rings in *trans*-fused ladder polysilanes increases, the onset wavelength of the $\sigma^* \leftarrow \sigma$ transition shifts to longer wavelengths. This progressive redshift reflects extended σ-conjugation, which lowers the HOMO–LUMO gap and yields significant oscillator strengths (f = 0.05–0.29) that corroborate enhanced delocalization in longer Si–Si frameworks.

Results and Discussion

In our siladecalin synthesis,[17] we found that salt metathesis of 1,2-dichlorocyclohexasilane **1** and dianion **2**Ph[30–35] allowed construction of the bicyclic framework of **3**Ph (Scheme 1a); the initially formed *cis*-**3**Ph major product could be equilibrated to the thermodynamically favored *trans*-**3**Ph diastereomer. This suggested the possibility of synthesizing a ladder tricyclohexasilane by simultaneous coupling of two equivalents of a dianion to a tetrafunctional cyclohexasilane like **4** (Scheme 2a). We anticipated not only employing dianion **2**Ph but also Marschner's dianion **2**TMS bearing trimethylsilyl substituents.[36]

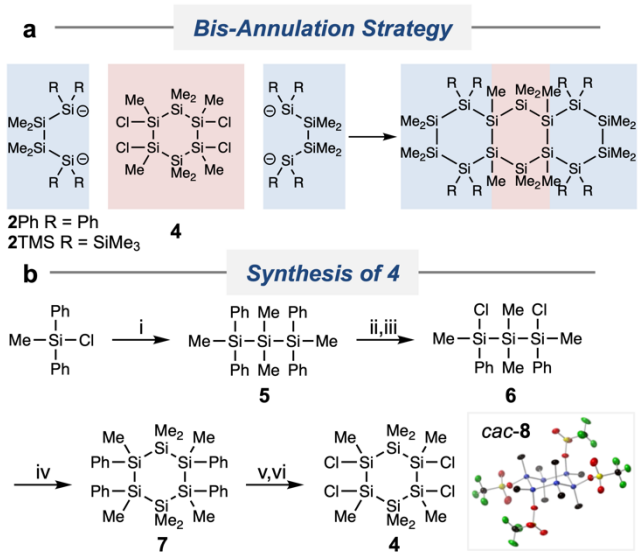

Scheme 2. A) Retrosynthesis: bis-annulation of tetrafunctional cyclosilane **4** to give tricyclo-Si_{14} scaffolds. B) Synthesis of cyclosilane **4.** i) Li, THF; *i*-PrMgCl; Cl_2SiMe_2, 78%; ii) F_3CSO_3H (2.0 equiv.), CH_2Cl_2 ; iii) NEt_3•HCl (2.0 equiv.), Et_2O, 92% (2 steps); iv) Na, toluene, 50%; v) F_3CSO_3H (4.4 equiv.), CH_2Cl_2; (vi) NEt_3•HCl (4.4 equiv.), Et_2O, 76% (2 steps).

Ultimately, we accomplished the synthesis of **4** in six steps from commercially available starting materials (Scheme 2b). $Ph_2MeSiCl$ was converted to the silyl lithiate[37] which was then coupled to Me_2SiCl_2 to give trisilane **5**. One phenyl ring was removed from each terminal silicon atom by triflic acid (F_3CSO_3H)[38–40] and the intermediate silyl triflate was converted to the more stable chlorosilane **6** by addition of triethylamine hydrochloride (NEt_3•HCl).[41] Chlorosilane **6** is known and was isolated as a ca. 1:1 mixture of two diastereomers, *meso* and *trans*. Trisilane **6** dimerized to the cyclohexasilane **7** upon reductive coupling initiated by Na. While **7** was isolated and carried forward as a mixture of diastereomers, two were separated by chromatography, and their relative configuration was assigned by X-ray crystallography (Figure S2). Finally, the remaining aromatic rings were removed by F_3CSO_3H, yielding **8**, which was converted to the chlorosilane **4** by reaction with NEt_3•HCl. A crystal structure of the major diastereomer *cac*-**8** was obtained (inset, Scheme 2b).

Having obtained the key tetrafunctional cyclosilane **4**, we first investigated the coupling of **4** with dianion **2**Ph. While a variety of reaction conditions were evaluated (Table S1), promising results were obtained when two equivalents of **2**Ph were added slowly to **4** as a solution in either benzene or toluene as a solvent at 0°C (Figure 1a). Higher temperatures did not increase the yield. After column chromatography, a mixture of at least two products was obtained that we were ultimately able to assign as predominantly the high symmetry *tst* and low symmetry *ct* diastereomers of ladder tricyclosilane **9**Ph (dr ca. 1:2 *tst:ct*, Figure 1b). The assignment of relative configuration arose from selective crystallization of pure diastereomers from different solvents: *tst*-**9**Ph recrystallized from toluene, while *ct*-**9**Ph recrystallized from hexanes. The crystals of *tst*-**9**Ph (block) and *ct*-**9**Ph (rod) were also of different morphologies (Figure S3). X-ray crystal structures of each diastereomer are shown in Figure 1c. While unidentified residual material could correspond to additional diastereomers, these could not be isolated in sufficient purity or quantity for definitive determination (Figure S4).

We next investigated the reactivity of dianion **2**TMS, which has been extensively employed by Marschner in the synthesis of cyclosilanes.[42,21] The reaction of **2**TMS with cyclosilane **1** yielded a new example of a siladecalin, *cis*-**3**TMS, in 82% yield and as a single diastereomer (Figure 1d). Assignment of relative configuration was based on the crystal structure (Figure 1e). The dianion **2**TMS therefore reacted with increased diastereoselectivity relative to **2**Ph: as we previously reported, *cis*-**3**Ph is the major product of the reaction between **1** and **2**Ph, but in 23:77 *trans:cis* dr and 50% yield.[17] Increased *cis* selectivity was also observed in the reaction between dianion **2**TMS and **4**, which yielded a different set of diastereomeric ladder tricyclosilanes than **2**Ph (Figure 1d). Instead of the *trans,syn,trans* (*tst*, minor) and *cis,trans* (*ct*, major) diastereomers observed with **2**Ph, the two isolated

diastereomers were the *cis,trans* (*ct*, major) and the *cis,anti,cis* (*cac*, minor). Structural assignments were made by recrystallization from the reaction mixture in toluene or tetrahydrofuran/methanol (Figure S5). Details of the recrystallization procedures are reported in the SI. We note that the purity of each isolated diastereomer was lower than for the **9**Ph series.

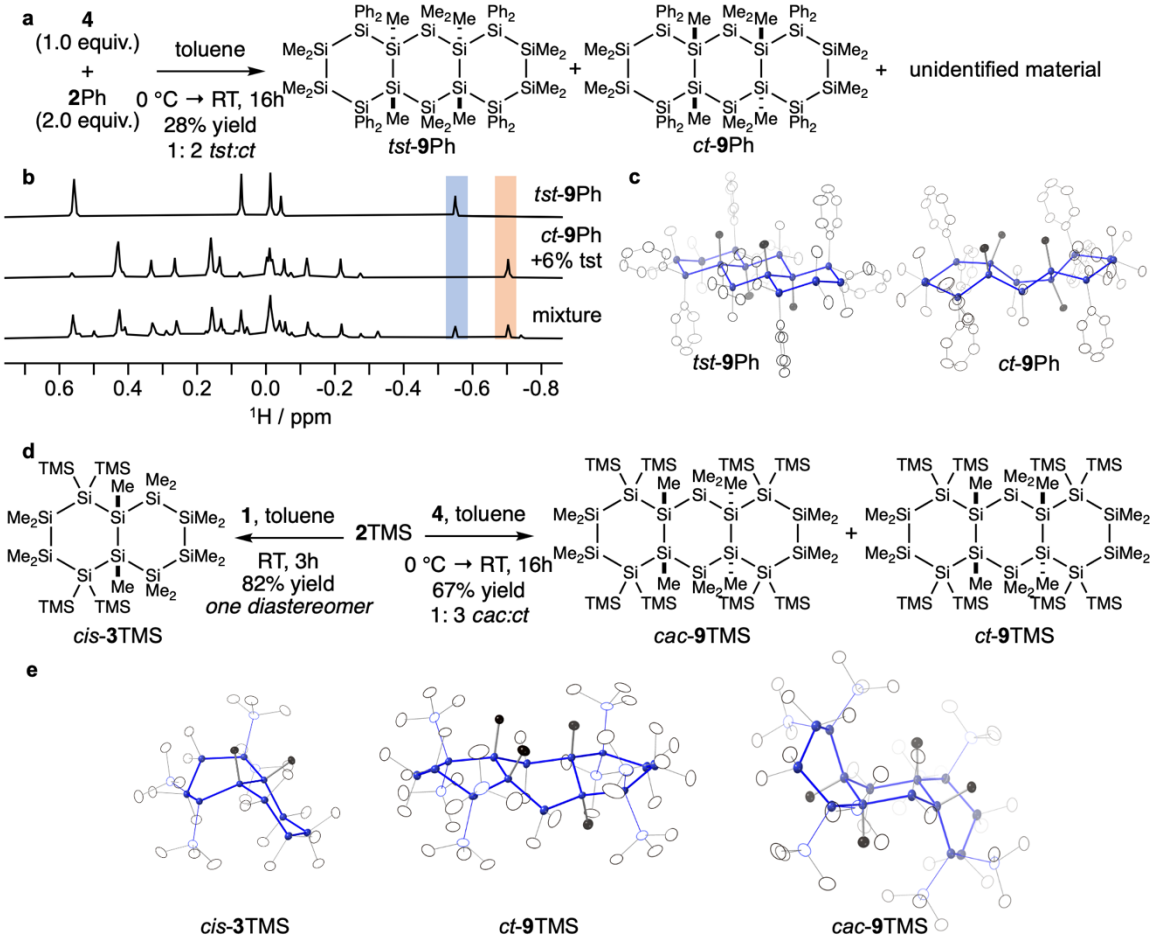

Figure 1. a) Synthesis of **9**Ph. b) Cropped ^{1}H NMR (400 MHz, $CDCl_3$) of the unpurified reaction mixture and pure *tst*- and *ct*-**9**Ph indicating a ca. 1:2 *tst:ct* diastereomeric ratio. c) X-ray crystal structures of *tst*-**9**Ph and *ct*-**9**Ph. Exocyclic substituents are shown in wireframe, with the exception of methyl groups at the stereogenic ring fusion silicon atoms. Solvent molecules, disorder, and hydrogens omitted for clarity. Displacement ellipsoids given at 50% probability level. Black = carbon; blue = silicon. d) Synthesis of **3**TMS and **9**TMS. e) X-ray crystal structures of *cis*-**3**TMS, *ct*-**9**TMS, and *cac*-**9**Ph. Exocyclic substituents are shown in wireframe, with the exception of methyl groups at the stereogenic ring fusion silicon atoms. Solvent molecules, disorder, and hydrogens omitted for clarity. Displacement ellipsoids given at 50% probability level. Black = carbon; blue = silicon.

To assess whether kinetic or thermodynamic factors govern the increased *cis* selectivity, we evaluated the relative stabilities of the diastereomeric products by calculating the ground state energies of the five possible diastereomers of **9**Ph and **9**TMS at the PBE0-D4/def2-TZVP (CPCM, Toluene) level of theory (Figure S6). For the TMS series, calculations revealed that *tat*-**9**TMS is the most thermodynamically stable diastereomer, although it was not isolated experimentally; in contrast, the experimentally isolated diastereomers, *ct*-9TMS and *cac*-**9**TMS, are higher in energy by +14.9 and +44.3 kJ mol-1, respectively. These energy differences strongly suggest that the high *cis* selectivity observed with dianion **2**TMS results from kinetic control. In contrast, for dianion **2**Ph, the experimentally isolated diastereomers *tst*-**9**Ph (ΔG = 0 kJ mol-1) and *ct*-**9**Ph (ΔG = +3.9 kJ mol-1) emerged as the two lowest-energy isomers. In our previous study of siladecalins, we observed that the addition of dianion **2**Ph equilibrated the initially formed *cis*-**3**Ph to the more stable *trans*-**3**Ph. This suggested the possibility that the isolation of *tst*-**9**Ph and *ct*-**9**Ph reflects thermodynamic control. Supporting this hypothesis, we found that reducing the reaction time between **2**Ph and **4** from 16 hours to 3 hours significantly increased the amount of the *ct* isomer relative to the *tst* (10:90 *tst:ct,* Figure S6).

However, the finding that dianion **2**Ph, but not **2**TMS, epimerizes a stereogenic silicon center complicates our understanding of the epimerization mechanism. In our synthesis of the siladecalins, we hypothesized that coordination of anionic **2**Ph to a stereogenic Si could transiently form a pentacoordinated silicate that could return to a tetrahedral geometry with either retention or inversion of configuration. This hypothesis was rooted in extensive prior work on the racemization of stereogenic-at-silicon silanes via hypervalent silicon.[43–46] However, it is unclear why **2**Ph and **2**TMS would differ in the ability to form a hypervalent silicon, suggesting that a different mechanism may be operative.

We hope these experimental findings will motivate further mechanistic studies. Conformational analysis of cyclohexanes and fused ring systems is foundational in natural product synthesis[47] and of clear, emerging relevance to complex inorganic molecular skeletons as well.[21] Moreover, configuration-dependent conformation impacts key properties, and we will show below that the *trans* configuration accessed under thermodynamic control results in interesting conformation-dependent light absorption.

We investigated how the onset of light absorption (λ_{onset}) changed with each additional ring. A redshift is observed for π-conjugated fused rings (linear acenes) from benzene to naphthalene to anthracene. Unlike the planar and rigid acenes, however, the ladder cyclohexasilanes are not planar. The photophysical properties of linear oligo- and polysilanes have long been appreciated to be conformation dependent, with the longest-wavelength light absorption occurring in an all-*anti* conformation.[18,48,49] The conformational diversity of the ladder tricyclohexasilanes is readily apparent from the X-ray crystal structures in Figure 1, which show multiple ring conformers, including chair, twist, and boat, sometimes within the same molecule. Prior computational[50] and experimental[51] work indicates that ring-inversion (e.g., chair-flipping) is much more rapid for cyclohexasilanes than cyclohexane.

We therefore became particularly interested in the comparison of monocyclic, bicyclic, and tricyclic compounds with a *trans* ring fusion as a well-defined homologous series in which the longest all-*anti* conformation would shift from 2 to 4 to 6 consecutive Si atoms (Figure 2a) if all rings adopted a chair conformation. The *cis* diastereomers necessitate a *gauche* conformation, resulting in shorter σ-conjugated pathways. In short, we would predict that λ_{onset} (reflecting a $\sigma^* \leftarrow \sigma$ HOMO–LUMO transition) should progressively increase with increasing rings within the *trans* series, but λ_{onset} within the *cis* series would minimally change with increasing rings due to gauche conformational defects. The simplified skeletons in Figure 2a correspond to the *ct*- and *tst*-**9**Ph skeletons isolated herein, as well as the monocyclic and bicyclic systems for which we have previously reported the synthesis and X-ray crystal structures,[32,33] suggesting an opportunity to validate the predicted trends.

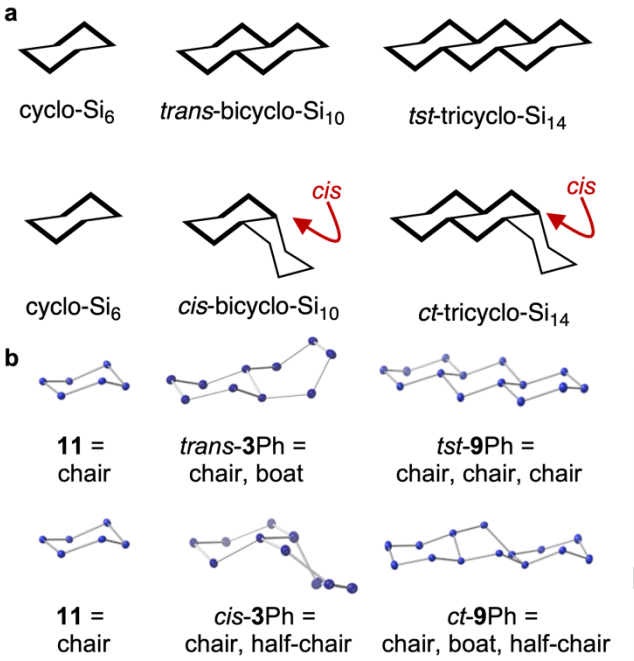

Figure 2. a) Simplified representations of the longest all-*anti* segments (highlighted in bold) in diastereomeric mono-, bi-, and tricyclic systems constrained to chair conformations. Any *cis* relative configuration introduces a gauche conformation.[52] b) Real solid-state cyclohexasilane conformations from X-ray crystal structures. All organic substituents omitted for clarity.

However, there are several confounding factors in real samples, including:

(1) The UV-vis spectra of phenyl-functionalized cyclosilanes contained an absorption band at ca. 280 nm, hypothesized to arise from the exocyclic phenyl rings, which obscured the conformation-dependent σ*←σ transitions of the Si–Si framework (Figure 3a, Figure S8). Multiple attempts to remove the phenyl rings were not successful. We previously reported the conversion of **11**Ph to **11**H [39] and the conversion of *cis*- and *trans*-**3**Ph to *cis*- and *trans*-**3**H[17] by Si–Ph *ipso*-selective protonolysis with F_3CSO_3H followed by Si–O_3SCF_3 reduction with $LiAlH_4$. However, the attempted comprehensive dearylation of *tst*-**9**Ph under a variety of conditions was always accompanied by Si–Si bond cleavage (Table S2, Figure S9). Prior work has documented Si–Si cleavage during related reactions[53,54] and has shown that in oligosilanes bearing multiple phenyl rings, the cleavage of the first phenyl group is fastest, as proximal triflate substituents deactivate further protonolysis.[55,56]

(2) The solid-state structures of the ladder cyclosilanes show that these structures do not exclusively adopt chair conformations. Only in the X-ray crystal structure *tst*-**9**Ph did all rings adopt a chair conformation; in *trans*-**3**Ph, one cyclosilane adopted a boat conformation (Figure 2b). While some of these distortions may arise from intermolecular π-π interactions in the solid state, it suggests that at room-temperature and in solution, the cyclosilanes could also deform away from the chair conformation.

(3) Real samples are not always diastereomerically pure: the dr's of the bicyclic *trans*-**3**Ph and *cis*-**3**Ph are 90:10 and 15:85 *trans:cis*, respectively. While *tst*-**9**Ph could be isolated as a single diastereomer, *ct*-**9**Ph still contained ca. 6% of the *tst* diastereomer; *tst*-**9**Ph and *ct*-**9**Ph have very similar absorption spectra, which may reflect contributions of the *tst* diastereomer to the overall spectrum (Figure S10).

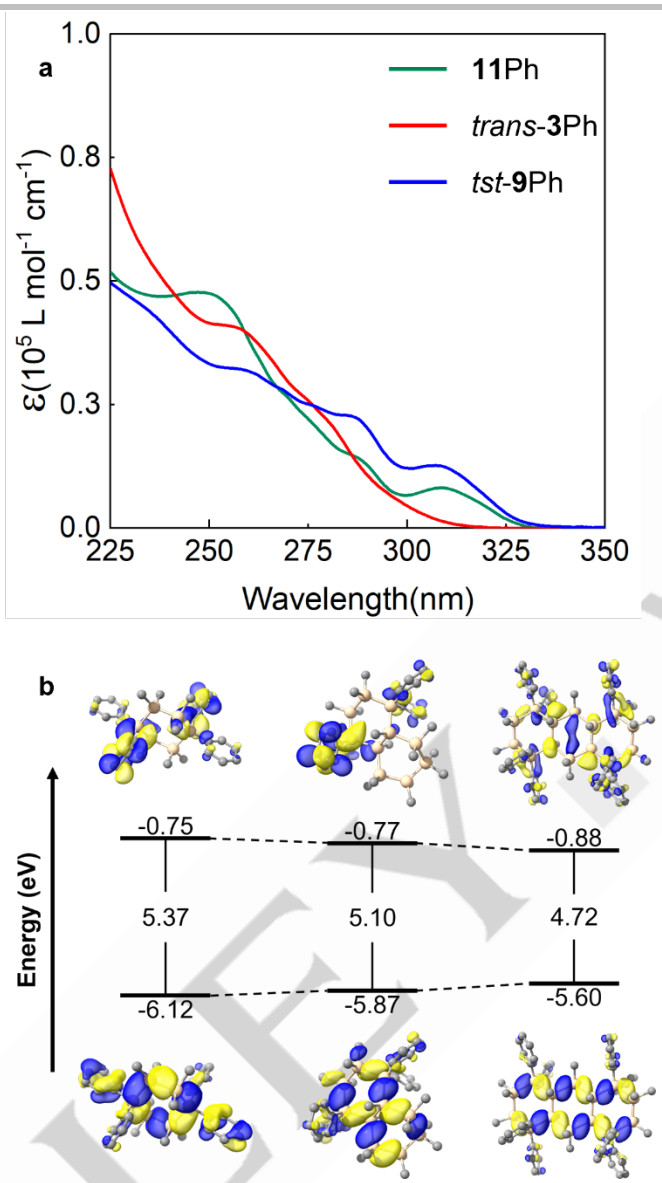

Figure 3. a) UV-vis spectra of **11**Ph, *trans*-**3**Ph, and *tst*-**9**Ph. Solvent = pentane, [compound] = 5×10^{-6} mol/L, room temperature. b) HOMO and LUMO plots of **11**Ph, *trans*-**3**Ph, and *tst*-**9**Ph and their associated energies (eV) calculated at the PBE0-D4/def2-TZVP (CPCM, Pentane) level of theory.

Since attempts to chemically remove the aromatic rings were not successful (*vide supra*), these structures were examined computationally, providing a robust framework for interpreting the complex experimental spectra. Time-dependent density functional theory (TD-DFT) was employed to gain deeper insight into the structure-property relationships of ladder polycyclosilanes by probing the nature of their electronic transitions. Calculations on both methyl- and phenyl-substituted systems allowed the inherent effects of extended σ-conjugation to be distinguished from substituent influences, effectively decoupling the contributions of the silicon framework from those of the aromatic π-system. Moreover, this computational approach enabled the analysis of pure diastereomers and conformers, thereby isolating intrinsic electronic effects that are often obscured in experimental samples.

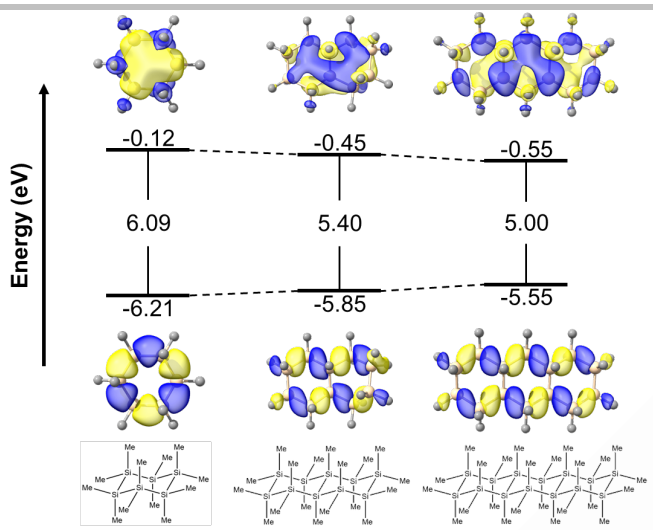

Figure 4. HOMO and LUMO plots of **11**Me, *trans*-**3**Me, and *tst*-**9**Me and their associated energies (eV) calculated at the PBE0-D4/def2-TZVP (CPCM, Pentane) level of theory.

TD-DFT analysis at the CAM-B3LYP-D3(BJ)/def2-TZVP (CPCM, Pentane) level of theory confirms that as the number of rings in *trans*-fused ladder polysilanes increases, the onset wavelength of the σ*←σ transition shifts to longer wavelengths (Table S3). In the methyl-substituted series (Figure 4), the lowest-energy excitation shifts from approximately 254 nm in the monocyclic (**11**Me) system to 281 nm in *trans*-**3**Me and further to 303 nm in *tst*-**9**Me. This progressive redshift reflects extended σ-conjugation, which lowers the HOMO–LUMO gap and yields significant oscillator strengths (f = 0.05–0.29) that corroborate enhanced delocalization in longer Si–Si frameworks.

In contrast, the phenyl-substituted ladder polysilanes exhibit markedly different spectral features due to the aromatic π-system. In this series (**11**Ph, *trans*-**3**Ph, and *tst*-**9**Ph), the computed lowest-energy transitions are symmetry-forbidden π*←σ excitations with negligible oscillator strengths (f = 1.0x10^{-7}) (Figure 3b). Notably, these weak states are nearly degenerate with higher-lying, allowed σ*←σ transitions that collectively produce the intense absorption band observed at 280 nm. This interplay indicates that although phenyl substitution extends effective conjugation through σ–π interactions and induces a redshift relative to the methyl-substituted systems, the allowed transitions of the silicon framework are effectively masked by the intense aromatic absorptions

Conclusion

Herein, we report the first examples of ladder tricyclohexasilanes by a double-annulation strategy employing a dianion and tetrafunctional cyclohexasilane. Four different examples, representing three of the five possible diastereomers, were isolated. We found that depending on the identity of the dianion and with a shorter reaction time, a pronounced *cis* diastereoselectivity was observed that yielded predominantly the *cis,trans* and *cis,anti,cis* diastereomers. With extended reaction times, the more thermodynamically stable *trans,syn,trans* diastereomer could be isolated. These results point to selectivity determined by kinetic versus thermodynamic control, supported by computational studies of relative diastereomer stability. At the same time, these data complicate an earlier model of thermodynamically-controlled epimerization based on transient formation of a pentavalent silicate; such a model would predict that dianions **2**Ph and **2**TMS should both result in epimerization, while our data show that only 2Ph leads to the *trans* ring fusion. More mechanistic understanding is need, as a combined experimental and theoretical study of light absorption in the homologous series of ladder compounds bearing the *trans* configuration (**11**Ph, *trans*-**3**Ph, and *tst*-**9**Ph) revealed extended σ-conjugation with each additional ring. We believe these results will motivate mechanistic study of stereomutation in complex cyclosilanes towards the goal of stereoselective synthesis of well-defined σ-chromophores.

Supporting Information

The authors have cited additional references within the Supporting Information.[57–65] The Supporting Information includes supplemental figures, experimental details, characterization data, and theoretical methods (NMR, X-ray crystallography) (PDF); X-ray crystallography files (CIF); raw NMR FIDs (ZIP); and computational coordinates (xyz).

Acknowledgements

This research was primarily supported by the U.S. Department of Energy (DOE), Office of Science, Basic Energy Sciences, under Award No. DE-SC0020681. X-ray crystallography was supported by the U.S. National Institutes of Health (NIH) under Award 1S10OD030352 (M.A.S). Research computing at MIT (Supercloud) is acknowledged for generous allocations of computing resources.

Keywords: silanes • ladder polymers • annulation • diastereoselectivity • conjugation

CCDC Deposition numbers 2427903 (tst-7), 2427904 (cac-8), 2427905 (cac-9TMS), 2427906 (cac-7), 2427907 (cis-3TMS), 2427908 (ct-9TMS), 2427909 (tst-9Ph), and 2427910 (ct-9Ph) contain the supplementary crystallographic data for this paper. These data are provided free of charge by the joint Cambridge Crystallographic Data Centre and Fachinformationszentrum KarlsruheDeposition Access Structures service.

[1] Y. C. Teo, H. W. H. Lai, Y. Xia, *Chemistry - A European Journal* **2017**, *23*, 14101–14112.
[2] J. A. M. Mercer, C. M. Cohen, S. R. Shuken, A. M. Wagner, M. W. Smith, F. R. Moss, M. D. Smith, R. Vahala, A. Gonzalez-Martinez, S. G. Boxer, N. Z. Burns, *Journal of the American Chemical Society* **2016**, *138*, 15845–15848.
[3] J. S. Sinninghe Damsté, M. Strous, W. I. C. Rijpstra, E. C. Hopmans, J. A. J. Geenevasen, A. C. T. Van Duin, L. A. Van Niftrik, M. S. M. Jetten, *Nature* **2002**, *419*, 708–712.
[4] Z. Chen, J. A. M. Mercer, X. Zhu, J. A. H. Romaniuk, R. Pfattner, L. Cegelski, T. J. Martinez, N. Z. Burns, Y. Xia, *Science* **2017**, *357*, 475–479.
[5] Z. Chen, X. Zhu, J. Yang, J. A. M. Mercer, N. Z. Burns, T. J. Martinez, Y. Xia, *Nature Chemistry* **2020**, *12*, 302–309.
[6] A. Schlüter, *Advanced Materials* **1991**, *3*, 282–291.
[7] E. R. McClure, P. Das, K. B. Idrees, D. Jung, O. K. Farha, J. A. Kalow, *Polymer Chemistry* **2023**, *14*, 4906–4911.
[8] J. Lee, A. J. Kalin, T. Yuan, M. Al-Hashimi, L. Fang, *Chem. Sci.* **2017**, *8*, 2503–2521.
[9] T. Ikai, S. Miyoshi, K. Oki, R. Saha, Y. Hijikata, E. Yashima, *Angew Chem Int Ed* **2023**, *62*, e202301962.
[10] C. Tang, X. Ma, J. Wang, X. Zhang, R. Liao, Y. Ma, P. Wang, P. Wang, T. Wang, F. Zhang, Q. Zheng, *Angew Chem Int Ed* **2021**, *60*, 19314–19323.
[11] H. Liang, K. Otsubo, Y. Wakabayashi, H. Sagayama, S. Kawaguchi, H. Kitagawa, *Angew Chem Int Ed* **2024**, *63*, e202400162.
[12] S. Matsuo, S. Nonaka, A. Mihata, K. Shikinaka, Y. Kaneko, *Polym. Chem.* **2025**, *16*, 850–857.
[13] W. L. Leong, J. J. Vittal, *Chemical Reviews* **2011**, *111*, 688–764.
[14] H. Matsumoto, H. Miyamoto, N. Kojima, Y. Nagai, *Journal of the Chemical Society, Chemical Communications* **1987**, 1316–1317.
[15] M. Unno, R. Tanaka, S. Tanaka, T. Takeuchi, S. Kyushin, H. Matsumoto, *Organometallics* **2005**, *24*, 765–768.
[16] S. Kyushin, Y. Ueta, R. Tanaka, H. Matsumoto, *Chemistry Letters* **2006**, *35*, 182–183.
[17] E. A. Marro, C. P. Folster, E. M. Press, H. Im, J. T. Ferguson, M. A. Siegler, R. S. Klausen, *Journal of the American Chemical Society* **2019**, *141*, 17926–17936.
[18] A. Bande, J. Michl, *Chemistry - A European Journal* **2009**, *15*, 8504–8517.
[19] R. L. Clarke, *Journal of the American Chemical Society* **1961**, *83*, 965–968.
[20] J. W. Cook, N. A. McGinnis, S. Mitchell, *Journal of the Chemical Society (Resumed)* **1944**, 286–293.
[21] K. E. Wentz, A. F. Gittens, R. S. Klausen, *J. Am. Chem. Soc.* **2025**, *147*, 2938–2959.
[22] Q. Jiang, A. F. Gittens, S. Wong, M. A. Siegler, R. S. Klausen, *Chem. Sci.* **2022**, *13*, 7587–7593.
[23] W. Yuan, C. He, *Synthesis* **2022**, *54*, 1939–1950.
[24] W. Yuan, X. Zhu, Y. Xu, C. He, *Angew Chem Int Ed* **2022**, *61*, e202204912.
[25] Y. Wu, L. Zheng, Y. Wang, P. Wang, *Chem* **2023**, *9*, 3461–3514.
[26] H. Zhou, R. Properzi, M. Leutzsch, P. Belanzoni, G. Bistoni, N. Tsuji, J. T. Han, C. Zhu, B. List, *J. Am. Chem. Soc.* **2023**, *145*, 4994–5000.
[27] J. J. Dalton, A. Bernal Sánchez, A. T. Kelly, J. C. Fettinger, A. K. Franz, *ACS Catal.* **2024**, *14*, 1005–1012.
[28] L. Wu, L. Zhang, J. Guo, J. Gao, Y. Ding, J. Ke, C. He, *Angew Chem Int Ed* **2024**, *63*, e202413753.
[29] M. A. Land, J. Bedard, G. Tanner, J. D. Masuda, S. S. Chitnis, *Angewandte Chemie International Edition* **2025**, DOI 10.1002/anie.202503568.
[30] E. A. Marro, E. M. Press, T. K. Purkait, D. Jimenez, M. A. Siegler, R. S. Klausen, *Chemistry - A European Journal* **2017**, *23*, 15633–15637.
[31] H. Wakefield, I. Kevlishvili, K. E. Wentz, Y. Yao, T. B. Kouznetsova, S. J. Melvin, E. G. Ambrosius, A. Herzog-Arbeitman, M. A. Siegler, J. A. Johnson, S. L. Craig, H. J. Kulik, R. S. Klausen, *J. Am. Chem. Soc.* **2023**, *145*, 10187–10196.
[32] E. A. Marro, E. M. Press, M. A. Siegler, R. S. Klausen, *J. Am. Chem. Soc.* **2018**, *140*, 5976–5986.
[33] E. M. Press, E. A. Marro, S. K. Surampudi, M. A. Siegler, J. A. Tang, R. S. Klausen, *Angew Chem Int Ed* **2017**, *56*, 568–572.
[34] H. Wakefield, S. J. Melvin, J. Jiang, I. Kevlishvili, M. A. Siegler, S. L. Craig, H. J. Kulik, R. S. Klausen, *Chem. Commun.* **2024**, *60*, 4842–4845.
[35] T. K. Purkait, E. M. Press, E. A. Marro, M. A. Siegler, R. S. Klausen, *Organometallics* **2019**, *38*, 1688–1698.
[36] C. Kayser, G. Kickelbick, C. Marschner, *Angew. Chem. Int. Ed.* **2002**, *41*, 989–992.
[37] H. Gilman, G. D. Lichtenwalter, *Journal of the American Chemical Society* **1958**, *80*, 608–611.
[38] W. Uhlig, *Journal of Organometallic Chemistry* **1991**, *402*, C45–C49.
[39] W. Uhlig, *Chemische Berichte* **1996**, *129*, 733–739.
[40] J. Y. Corey, D. M. Kraichely, J. L. Huhmann, J. Braddock-Wilking, A. Lindeberg, *Organometallics* **1995**, *14*, 2704–2717.

[41] T. A. Su, H. Li, M. L. Steigerwald, L. Venkataraman, C. Nuckolls, *Nature Chemistry* **2015**, *7*, 215–220.
[42] R. Fischer, T. Konopa, S. Ully, J. Baumgartner, C. Marschner, *Journal of Organometallic Chemistry* **2003**, *685*, 79–92.
[43] L. H. Sommer, *Stereochemistry, Mechanism, and Silicon: An Introduction to the Dynamic Stereochemistry and Reaction Mechanisms of Silicon Centers*, McGraw-Hill, New York, **1965**.
[44] L. H. Sommer, P. G. Rodewald, *J. Am. Chem. Soc.* **1963**, *85*, 3898–3899.
[45] M. Oestreich, G. Auer, M. Keller, *Eur J Org Chem* **2005**, *2005*, 184–195.
[46] E. P. A. Couzijn, J. C. Slootweg, A. W. Ehlers, K. Lammertsma, *J. Am. Chem. Soc.* **2010**, *132*, 18127–18140.
[47] R. Chen, Y. Shen, S. Yang, Y. Zhang, *Angew Chem Int Ed* **2020**, *59*, 14198–14210.
[48] R. D. Miller, D. Hofer, J. Rabolt, G. N. Fickes, *J. Am. Chem. Soc.* **1985**, *107*, 2172–2174.
[49] A. Fukazawa, H. Tsuji, K. Tamao, *J. Am. Chem. Soc.* **2006**, *128*, 6800–6801.
[50] G. Tekautz, A. Binter, K. Hassler, M. Flock, *ChemPhysChem* **2006**, *7*, 421–429.
[51] D. Casarini, L. Lunazzi, A. Mazzanti, *J. Org. Chem.* **1998**, *63*, 9125–9127.
[52] J. Michl, R. West, *Acc. Chem. Res.* **2000**, *33*, 821–823.
[53] A. Fukazawa, H. Tsuji, K. Tamao, *Silicon Chem* **2007**, *3*, 157–163.
[54] U. Herzog, R. West, *Macromolecules* **1999**, *32*, 2210–2214.
[55] K. Matyjaszewski, Y. L. Chen, *Journal of Organometallic Chemistry* **1988**, *340*, 7–12.
[56] K. E. Ruehl, K. Matyjaszewski, *Journal of Organometallic Chemistry* **1991**, *410*, 1–12.
[57] R. Fischer, D. Frank, W. Gaderbauer, C. Kayser, C. Mechtler, J. Baumgartner, C. Marschner, *Organometallics* **2003**, *22*, 3723–3731.
[58] F. Neese, *WIREs Comput Mol Sci* **2012**, *2*, 73–78.
[59] F. Neese, *WIREs Comput Mol Sci* **2022**, *12*, e1606.
[60] C. Adamo, V. Barone, *The Journal of Chemical Physics* **1999**, *110*, 6158–6170.
[61] E. Caldeweyher, S. Ehlert, A. Hansen, H. Neugebauer, S. Spicher, C. Bannwarth, S. Grimme, *The Journal of Chemical Physics* **2019**, *150*, 154122.
[62] F. Weigend, R. Ahlrichs, *Phys. Chem. Chem. Phys.* **2005**, *7*, 3297.
[63] V. Barone, M. Cossi, *J. Phys. Chem. A* **1998**, *102*, 1995–2001.
[64] F. Weigend, *Phys. Chem. Chem. Phys.* **2006**, *8*, 1057.
[65] T. Yanai, D. P. Tew, N. C. Handy, *Chemical Physics Letters* **2004**, *393*, 51–57.

Entry for the Table of Contents

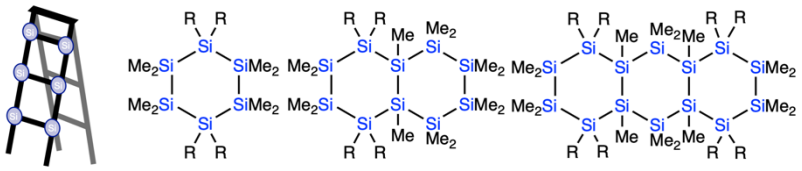

Herein, we report the synthesis of a homologous series of ladder cyclohexasilanes containing 1, 2, or 3 fused rings. The tricyclosilanes rank among the most architecturally and stereochemically complex oligosilanes yet synthesized. A combined experimental and theoretical study suggested that the diastereoselectivity in a key annulation is governed by kinetic control. This study also revealed extended σ-conjugation with each additional ring within the all-*trans* ladder cyclosilanes series.

Institute and/or researcher Twitter usernames: @Klausen_Group